Influence of Molybdenum, Zircon and Copper on Structure of Aluminum Alloy AlSi10Mg(Cu) (En Ac-43200)

Dana Bolibruchová[1], Peter Hajdúch[2], Marek Brůna[1]
[1]Department of technological engineering, University of Žilina, Univerzitná 1, 010 26 Žilina, Slovakia. E-mail: danka.bolibruchova@fstroj.uniza.sk
[2]Nemak Linz, Zeppelinstrasse 24, 4030 Linz, Austria

The paper deals with the influence of molybdenum, zirconia and cobalt on the AlSi10Mg (Cu) alloy microstructure. The work methodology was focused on the analysis of phases morphology for material alloyed with Mo, Zr and Co. Molybdenum in the AlSi10MgCu alloy creates phases with skeletal morphology bounded on iron phases Al(Fe, Mn, Mo)Si. Used heat treatment has softened these phases and is a prerequisite for increasing the strength characteristics and hardness. By alloying the alloy with zirconium to isolate Al3Zr phases, which represent a strong nucleation potential for α-Al. It has been confirmed that Al3Zr particles do not tend to interact with other elements. The results of experiments show that cobalt affects the morphology of iron phases. The findings of this study can provide further insight into the transition metals in Al-Si-Mg-Cu alloys and the potential for developing a new generation of heat-resistant alloys based on Al-Si.

Keywords: AlSi10Mg(Cu), (EN AC-43200), Mo, Zr, Co, SEM, EDX phase mapping

1 Introduction

AlSi10Mg (Cu) alloys belong to alloys with near eutectic composition, with good casting properties. They are mainly used for car parts characterized by thin walls and complex geometry. Castings have excellent mechanical and dynamic properties. For the above reasons, they are used for applications requiring high loads and combination of good thermal properties and low weight. Castings of these alloys are heat-treated by the T6 process [1]. AlSi10Mg (Cu) alloys are characterized by the presence of two, Al-Si and Al-Si-Cu eutectics, which are responsible for defining the microstructure and mechanical properties.

Attempts of current castings manufacturers for the automotive industry is the production of castings working in high temperatures. Motor operation is accompanied by a cyclic load during engine heating and cooling, this induces local pressure stresses and causes material deformation. Current Al-Si alloys (Mg, Cu) have a normal operating temperature up to 200 ° C. At higher temperatures, dissolving and / or thickening of reinforcing particles (e.g., rich on Cu and Mg) can adversely affect mechanical properties. Advances in fuel economy and performance of the combustion engine system have led to an increase in engine operating temperature and pressure, indicating the need to develop new creep-resistant aluminum alloys. One approach to the development of high-temperature alloys could allow for the formation of thermally stable intermetallic phases formed within the α-Al grains. Some transition metals (such as Mo, Zr, V, Co and Sc) due to their slow diffusion capacity into α-Al, low solubility with the possibility of formation of the trialuminide phase in the α-Al matrix can bring significant influence on the stability of the strength properties of aluminum alloys [2, 3]. However, the effect of transition metals in Al-Si alloys is limited due to their relatively low solubility in α-Al, leading to a low proportion of transition metal-rich precipitates after heat treatment. Particles rich in transition metals, such as Al3Zr, are mostly concentrated in α-Al. Precipitates rich in transition elements tend to be distributed unevenly throughout the microstructure because the distribution coefficient k0> 1 (e.g., for the binary system Al-Zr).

Alloys with a higher alloying amount may cause difficulties during casting because they require a higher melting temperature. Addition of the appropriate quantities of transition metals to Al-Si alloys is also carried out for better grain refinement (inoculation), e.g. Al-Ti-B. However, the combined presence of elements creating the perithectic (Zr, V) and B, can lead to their interactions, which may affect the effectiveness of the inoculation [2, 4, 5].

Rakhmonov et al. [2] in their AlSi7Cu0.3Mg alloy study found that when 0.12 wt. % Zr was added, the Al3Zr particles precipitated primarily to promote the refining effect of the α-Al matrix. These particles do not contain Si or Ti. However, a small amount of Al3Zr particles precipitating in the early stages of solidification reacts with Si and Ti. Interaction of Zr with these elements can weaken the effect of the Al3Zr particles and thus impair the strength properties of aluminum alloys. Accordingly, the amount of Zr is a determining factor in the appropriate alloying of Al-Si alloys to prevent the formation of unwanted intermetallic phases (AlSi)3(ZrTi) in the form of plates. From a literary survey [6, 7] it follows that Zr influences the development of the Al-Si alloys microstructure, and it has been shown that Zr, depending on the morphology of the Zr-phase, can increase or decrease the mechanical properties. The authors claim that the addition of Zr must not exceed 0.2 wt. % Zr. If the amount of Zr is high, coarsed primary Al3Zr phases will be formed and they will degrade the mechanical properties of the aluminum alloys. Medved et al. [7] reported that the addition of Zr to the analyzed material caused a change of the Cu-phase morphology from Chinese script form to plate or flake-like shape. After the heat treatment T6 was applied, the morphology changed to Chinese script form.

According to literary sources [8], the addition of 0.2 wt. % Zr to the AlSi9Cu3(Fe) alloy led to an increase in the α-Al phase formation temperature due to the formation of the Al3Zr phase, acting as a nucleant. The authors also claim that the heat treatment T6 does not affect the formation of Zr-phases since these phases occur at higher temperatures than the T6 [8]. Authors [9] investigated the effect of adding Mo and Mn into a Al-Si-Cu-Mg alloy. These two elements have the opposite partition coefficient (kMo> 1 and kMn <1). Mo (without Mn) formed coherent α-Al(Fe, Mo)Si phases with stoichiometric formulas in Al22(Fe1-3Mn4-6Mo)Si4, which were mostly found in interdendritics areas. Subsequent addition of Mn increased the number of phases by replacing the Fe atoms. The combined addition led to a more even distribution of phases in the microstructure. The authors state that as a result, the resistance to creep in the temperature range of 300 to 350 ° C has greatly improved. The influence of Co, Ni and Sr on the AlSi7 type was studied by the authors [10]. The results indicate that the combined effect of Co and Ni modifies eutectic Si. Sr significantly influences (shortens) the Co and Ni-rich phases. The combined Co and Ni addition has a good potential to increase the mechanical properties of the alloy examined at higher temperatures.

An analysis of the current state of knowledge derive some facts that have been confirmed by several authors, but there are a number of phenomenon which are not sufficiently / or never examined. Therefore, the aim of this paper is to analyze the phases formed in the AlSi10MgCu alloy by using Zr, Mo and Co.

2 Methodology of experiments

The alloy EN AC-43200 (Table 1) was used for experimental casts. The alloy has been pre-modified by the manufacturer. In order to increase the temperature resistance of the alloy, Mo, Zr and Co were added to the basic alloy (labeled as A - Table 2) in the form of master alloys. Samples labeled B, C, D (Table 2) were alloyed with 0.15 wt. % Mo, 0.15 wt. % Zr and last, 0.1 wt. % Co was added. The alloy was melted at Nemak Slovakia, s.r.o. in Striko furnace and maintained in an electric resistance furnace. The melt was then alloyed with mentioned elements at 770 ± 5 ° C and subsequently degassed by rotary degassing for 12 minutes. The density index ranged from DI = 1.00% to DI = 1.5%. The test samples were cast at a temperature of 760 to 770 ° C into a metal mold at 300 to 320 ° C, then samples were subjected to a heat treatment consisting of annealing at 530 ± 5 °C for 6 hours and cooling in water at 80 ± 5 ° C. Subsequently, artificial aging was carried out at 200 ± 5 °C for 3 hours. [11].

A scanning microscope (SEM) was used to analyze the resulting phases. The resulting intermetallic phases were evaluated by EDX analysis and phase separation on the examined area by mapping. Each specimen was examined in casted state and also after heat treatment.

Tab. 1 *Chemical composition of AlSi10Mg(Cu)/EN AC-43200 by ST EN 1706 [1]*

Element	Si	Fe	Cu	Mn	Mg	Ni	Zn	Pb	Ti	Al
wt. %	9.0-11.0	0.65	0.35	0.55	0.2-0.45	0.15	0.35	0.1	0.2	rest

Tab. 2 *Chemical composition of experimental samples*

Alloy	label	Si	Mg	Cu	Ti	Sr	Mn/Fe	Zr	Mo	Co
		wt. %								
AlSi10MgCu	A	9.39	0.38	0.30	0.12	0.014	0.861	0.0039	0.0002	0.0032
AlSi10MgCu+0,15 Mo	B	10.23	0.47	0.29	0.10	0.022	0.909	0.0042	0.1496	0.0031
AlSi10MgCu+0,15Mo+0,15Zr	C	9.23	0.37	0.28	0.11	0.015	0.844	0.128	0.1514	0.0029
AlSi10MgCu+0,15Mo+0,15Zr+0,1Co	D	9.16	0.37	0.28	0.11	0.015	0.835	0.134	0.151	0.094

3 Evaluation of experiments and discussion of results

AlSi10MgCu - sample A (no alloying elements, no heat treatment)

Phase deposition was investigated on SEM - Fig. 1, a detail from the EDX spot analysis area is shown in Fig. 2. Small intermetallic phases and coarse skeleton phases can be observed on the EDX sample. In the non-alloyied alloy there are "classical" iron-based intermetallic phases with skeletal morphology (indicated by a green arrow) and morphology of the so-called "Chinese script" (indicated by a yellow arrow). An Sr-based phase was also analyzed. This phase did not melt in the melting process and probably did not participate in the modification process. It has created a damaging needle-like morphology (indicated by a red arrow).

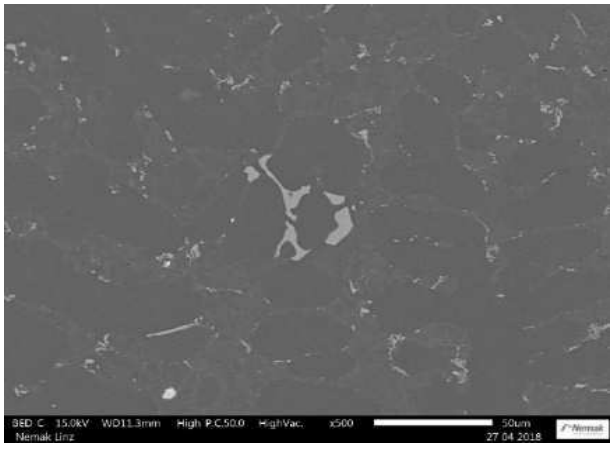

Fig. 1 *Phase morphology of AlSi10MgCu alloy (no alloying elements, no heat treatment) – sample A, SEM*

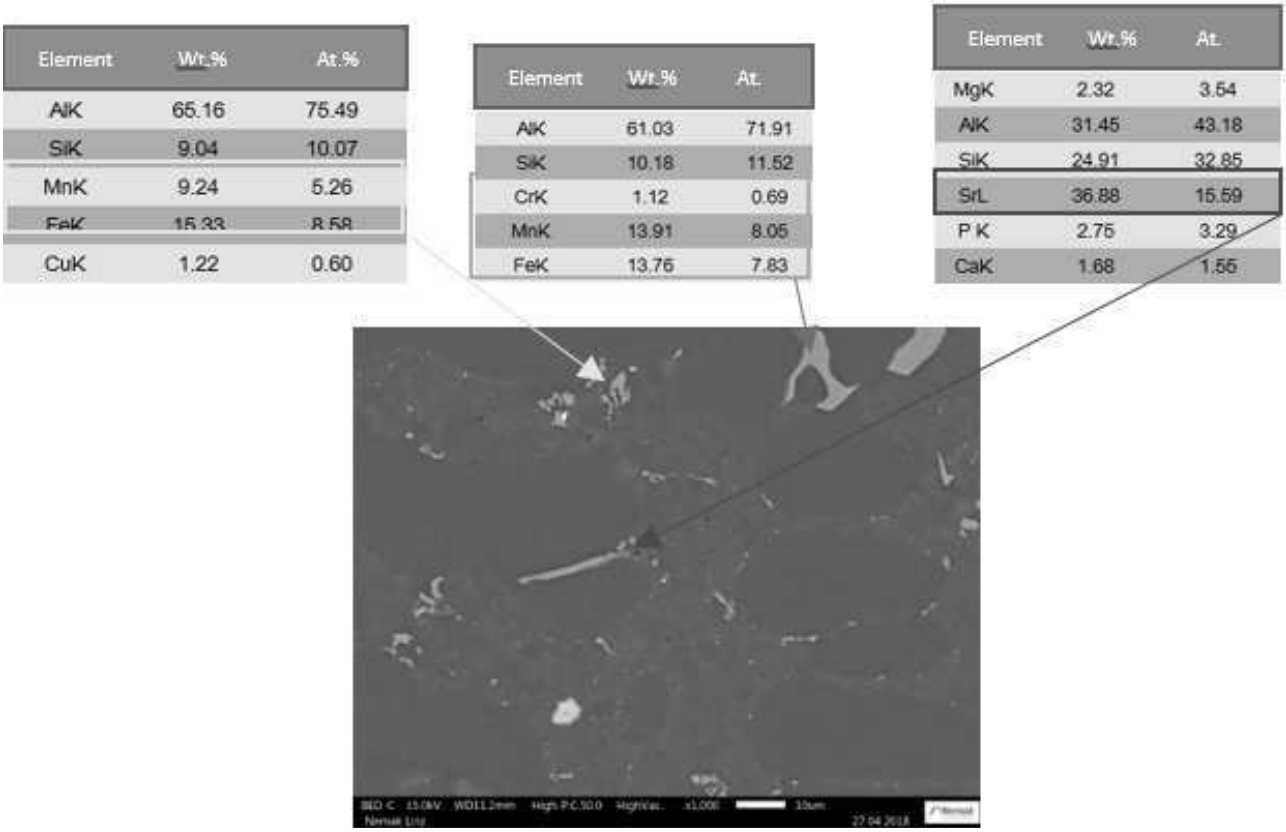

Fig. 2 *EDX analysis of AlSi10MgCu alloy phases, (no alloying elements, no heat treatment) (detail of figure 1) - sample A, SEM*

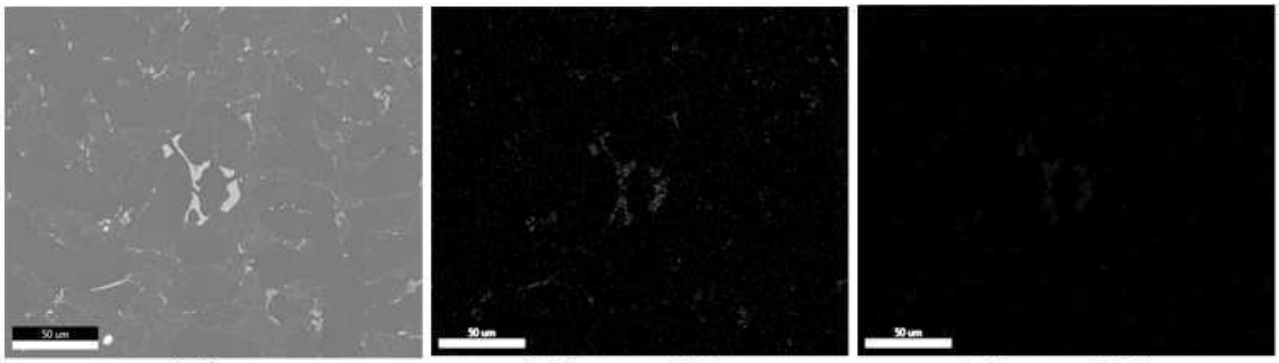

Fig. 3 *Phases mapping of AlSi10MgCu alloy (no alloying elements, no heat treatment) – sample A*

The distribution of the elements obtained by mapping (Figure 3) points to the truth of the claim that the coarse skeleton phase is based on Fe and Mn content, most likely being the Al15(FeMn)3Si2 phase.

AlSi10MgCu - sample A (non-legged alloy), heat treated

As can be seen from the picture (Figure 4), the heat treatment significantly refined the intermetallic phases. The iron phases Al15(FeMn)3Si2 changed the morphology from the skeleton formations to the Chinese script and strontium were globalized (Figure 5). Mapping pointed to the refining of Fe-based phases (Figure 6).

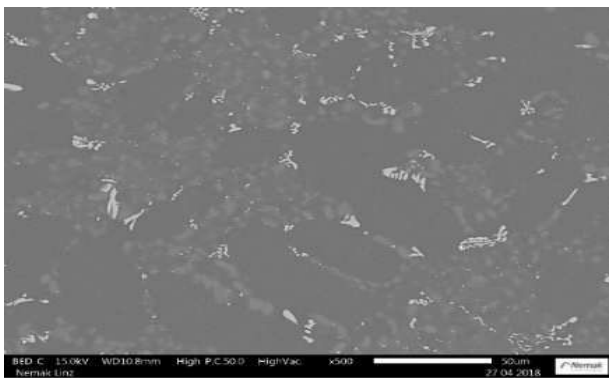

Fig. 4 *Phase morphology of AlSi10MgCu alloy (no alloying elements, with heat treatment) – sample A, SEM*

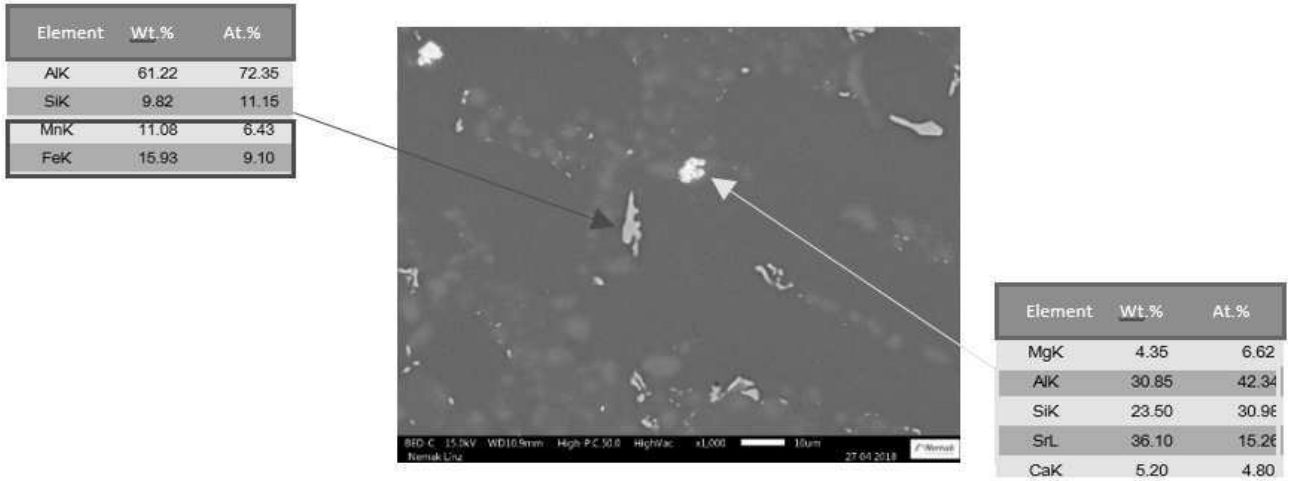

Fig. 5 *EDX analysis of AlSi10MgCu alloy phases, (no alloying elements, with heat treatment) (detail of figure 4) - sample A, SEM*

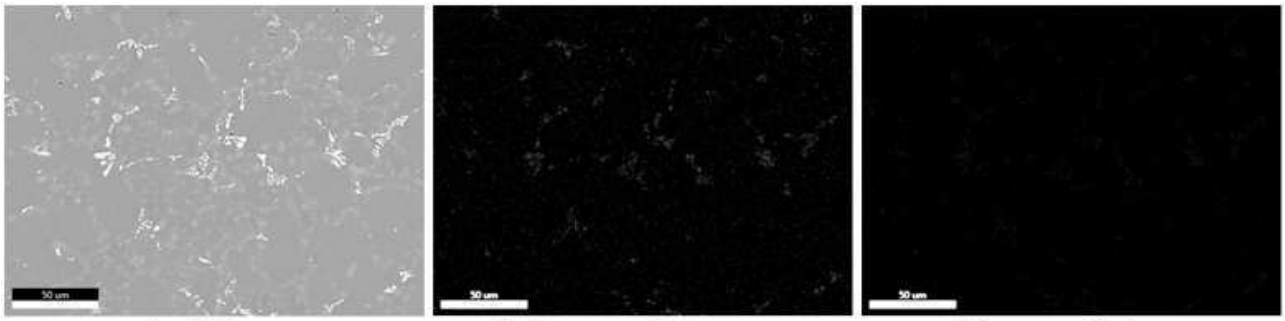

Fig. 6 *Phases mapping of AlSi10MgCu alloy (no alloying elements, with heat treatment) – sample A, SEM*

AlSi10MgCu + 0.15 wt. % Mo, sample B, without heat treatment

SEM in the investigated alloy pointed out the existence of skeletal phases (Figure 7a) and the mapping of the individual phases is shown in Fig. 4. It can be stated that the skeleton phases are based on Al(Fe, Mn, Mo)Si. The addition of Mo did not significantly affect the morphology of the phases compared to the non-alloyed material (see Figure 3).

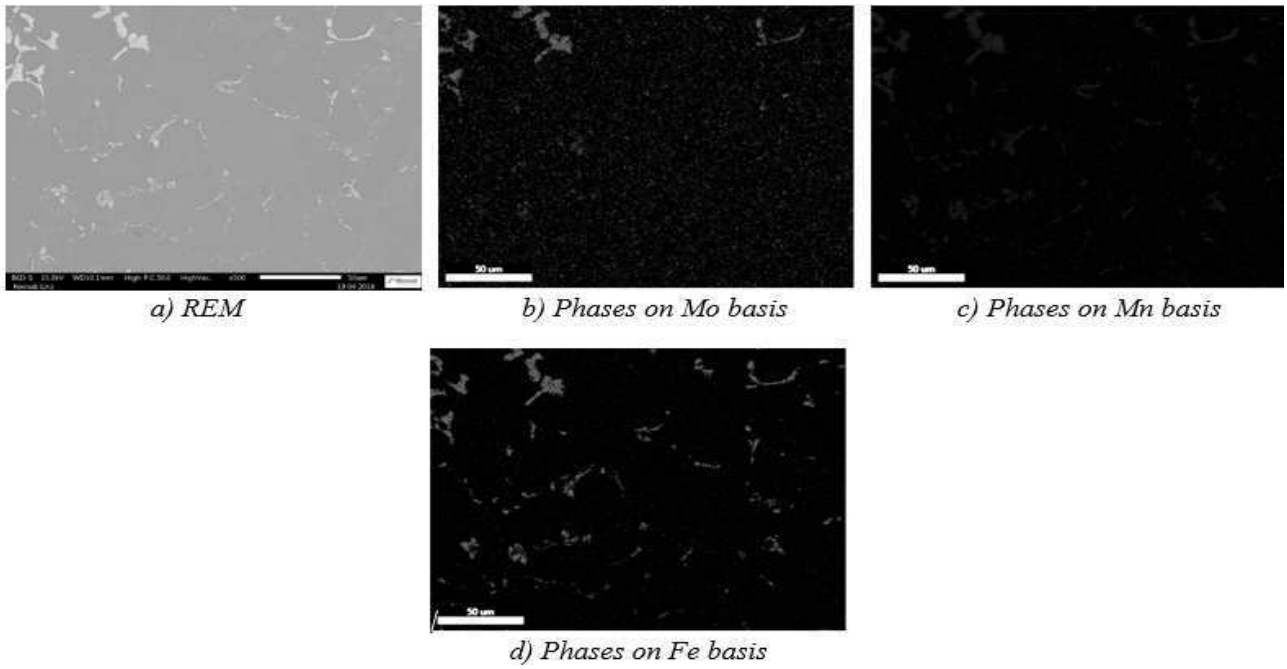

Fig. 7 *Phases mapping of AlSi10MgCu alloy with 0.15 wt. % Mo (exact amount of Mo – 0.1496 wt. %), without heat treatment - sample B, SEM*

AlSi10MgCu + 0.15 wt. % Mo, sample B, heat treated

In the studied alloy, the refined Al(Fe, Mn, Mo)Si (indicated by a red arrow) phase were observed, needles of Al5FeSi phases (indicated by a green arrow) and imperfect polyhedron phases based on Fe (marked with a yellow arrow) was also observed – fig. 8. When analyzing the influence of heat treatment on analyzed alloy, it can be confirmed that the heat treatment cycle significantly refined the skeleton phases of Al(Fe, Mn, Mo)Si (Figure 9) versus the alloy without the use of heat treatment (see Figure 7).

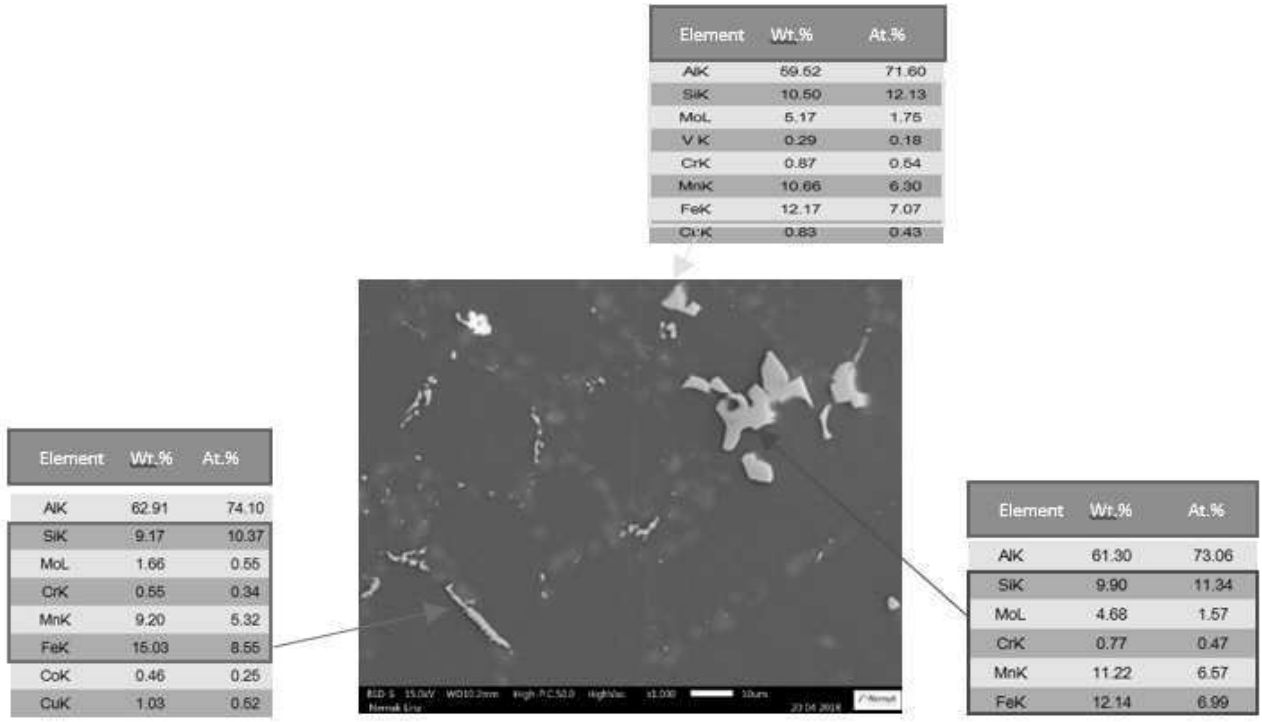

Fig. 8 *EDX analysis of AlSi10MgCu alloy with 0.15 wt. % Mo (exact amount of Mo – 0.1496 wt. %), without heat treatment - sample B, SEM*

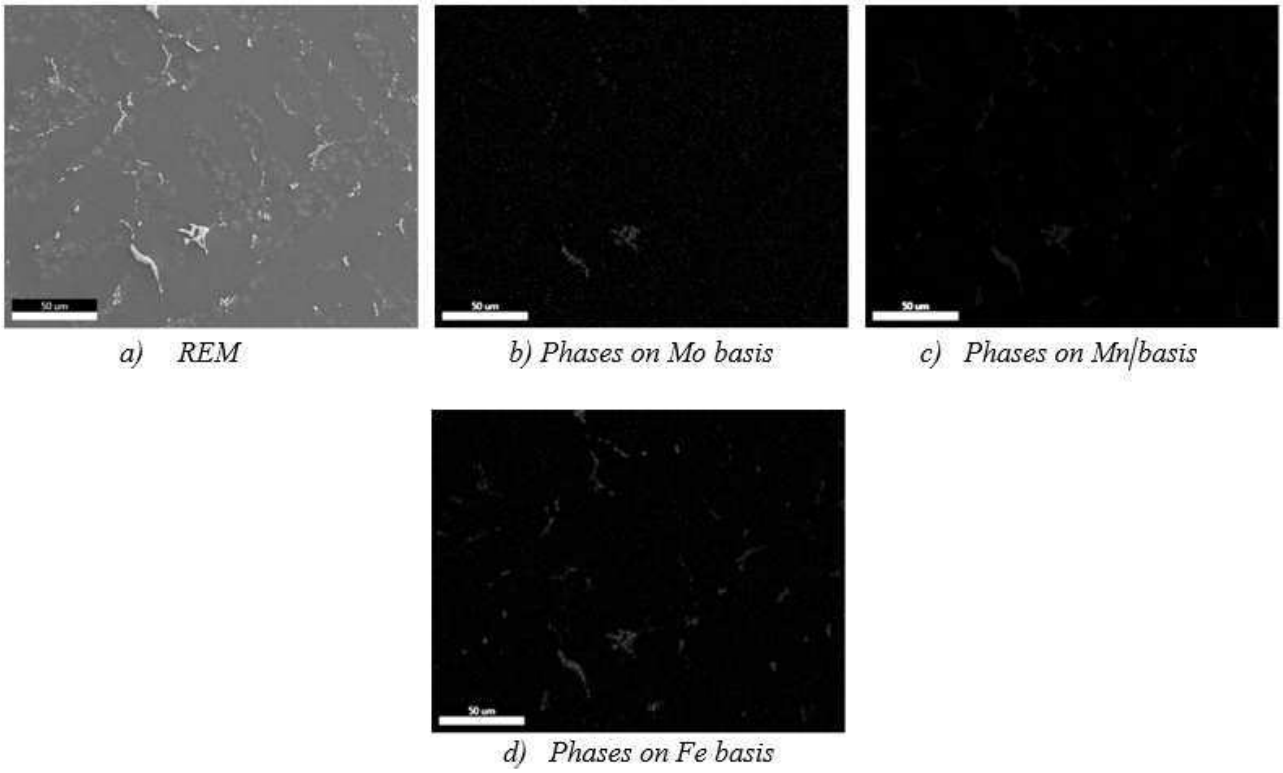

Fig. 9 *Phases mapping of AlSi10MgCu alloy with 0.15 wt. % Mo (exact amount of Mo – 0.1496 wt. %), with heat treatment - sample B, SEM*

AlSi10MgCu + 0.15 wt. % Mo + 0.15 wt. % Zr, sample C, no heat treatment

By adding 0.15 wt. % Zr to the AlSi10MgCu alloy with a synergistic effect of 0.15 wt. % Mo, the Al3Zr plate-like phase (indicated by the red arrow) was created. Mo formed only short phases of Al(Fe, Mn, Mo)Si type (marked with a yellow arrow) - Fig. 10.

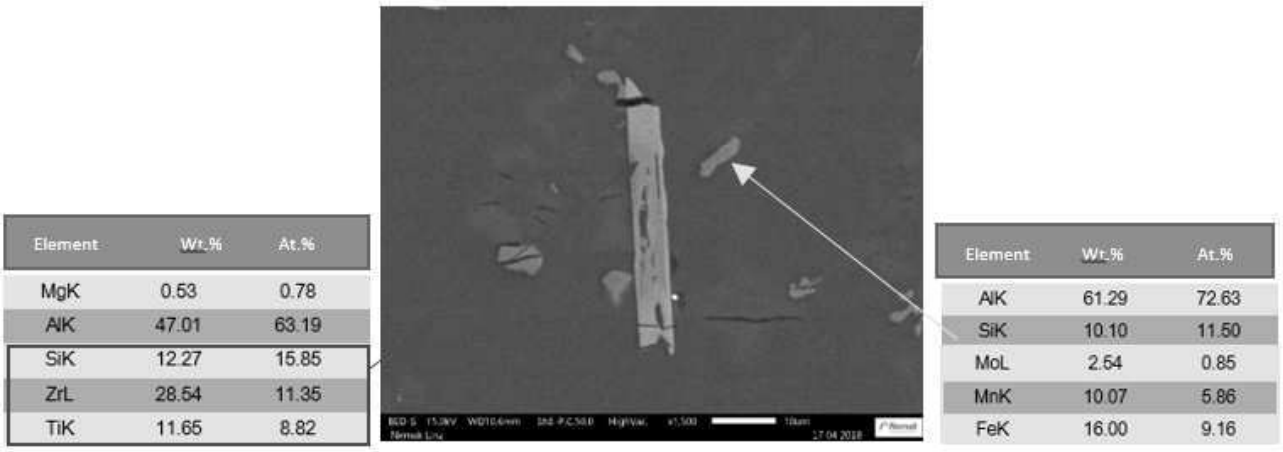

Fig. 10 *EDX analysis of AlSi10MgCu alloy with 0.15 wt. % Mo and 0.15 wt. % Zr (exact amount of Mo – 0.1496 wt. %, Zr – 0.128 wt. %), without heat treatment - sample C, SEM*

Phase distribution is described by mapping (Figure 11). From the picture, it can be stated that the synergistic effect of Mo and Zr caused the refining of the phases compared to the alloys without the use of Zr.

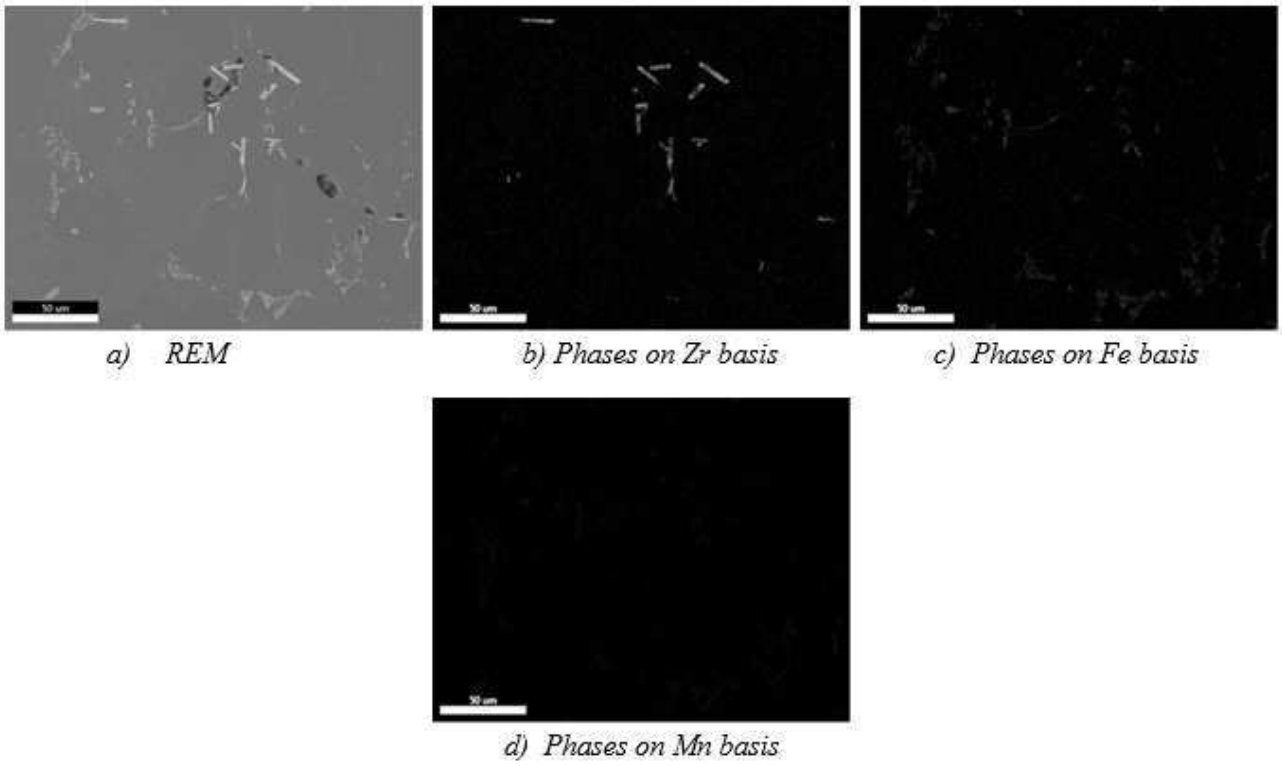

Fig. 11 *Phases mapping of AlSi10MgCu alloy with 0.15 wt. % Mo and 0.15 wt. % Zr (exact amount of Mo – 0.1496 wt. %, Zr – 0.128 wt. %), without heat treatment - sample C, SEM*

AlSi10MgCu + 0.15 wt. % Mo + 0.15 wt. % Zr, sample C, heat treated

After the heat treatment of the examined alloy, the plate-like phases were fragmented (Figure 12), it is probably Al(Fe, Mn, Mo)Si phase type (marked with a red arrow) and Al3Zr phases were markedly shortened (indicated by a yellow arrow). The distribution of the fragmented phases is shown in fig. 13.

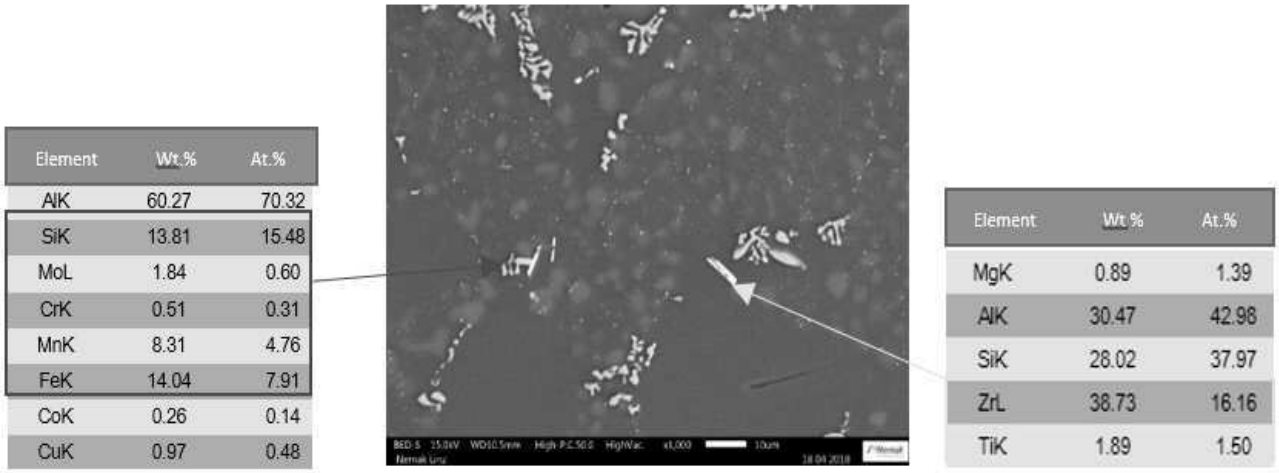

Fig. 12 *EDX analysis of AlSi10MgCu alloy with 0.15 wt. % Mo and 0.15 wt. % Zr (exact amount of Mo – 0.1514 wt. %, Zr – 0.128 wt. %), with heat treatment - sample C, SEM*

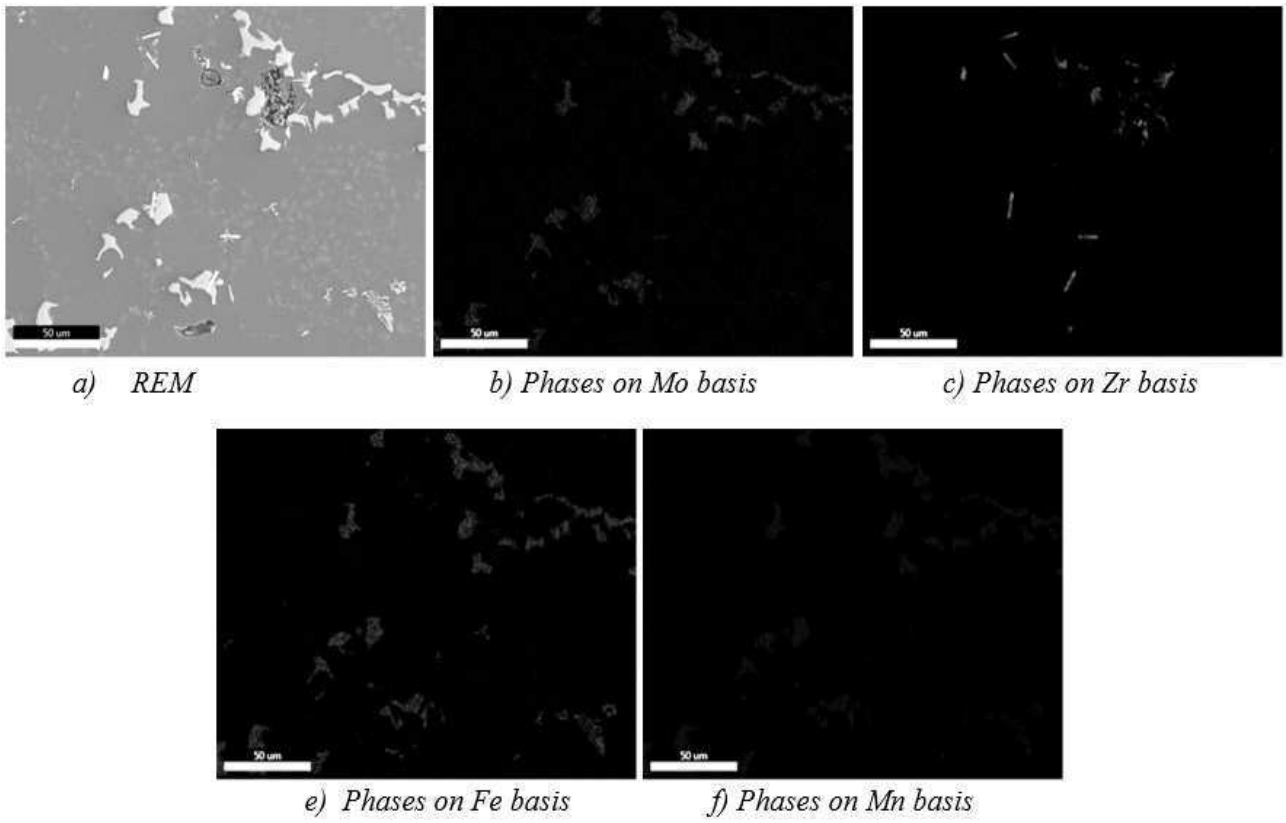

Fig. 13 *Phases mapping of AlSi10MgCu alloy with 0.15 wt. % Mo and 0.15 wt. % Zr (exact amount of Mo – 0.1514 wt. %, Zr – 0.128 wt. %), with heat treatment - sample C, SEM*

AlSi10MgCu + 0.15 wt. % Mo + 0.15 wt. % Zr + 0.1 wt. % Co, sample D, without heat treatment

After addition of 0.1 wt. % Co the morphology of the iron phases changed from the skeleton morphology to the Chinese script morphology (Figure 14) - (marked with a red arrow). The structure also revealed the undissolved Sr phase marked with a green arrow. It can be assumed that the used alloying elements affect the action of strontium in the alloy. The complex effect of alloying elements also affected the morphology of the Zr-phase. As can be seen in fig. 14 - marked with a purple arrow, the Zr-phase does not form a compact plate but is partially fragmented in a needle shape.

Mapping (Figure 15) clearly confirmed the significant refinement of Al3Zr and coursing of Al(Fe, Mn, Mo)Si compared to alloy with only two elements (see Figure 13).

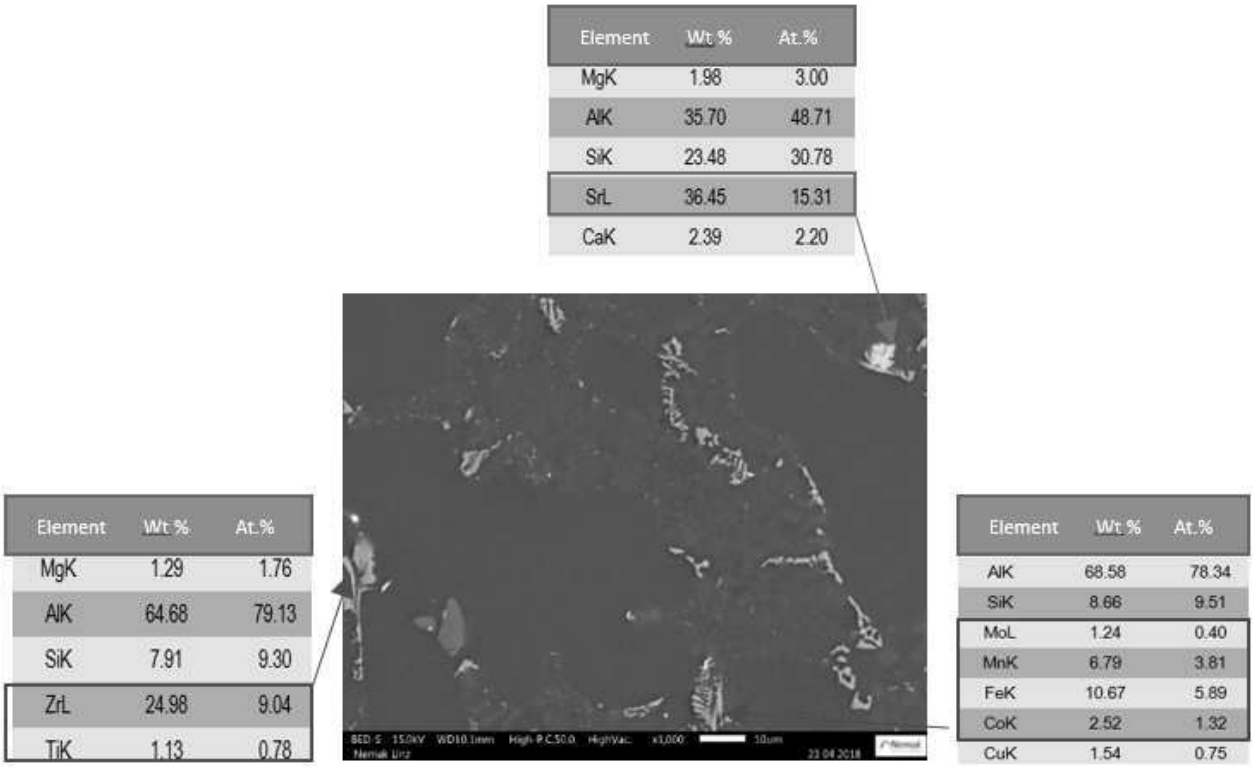

Fig. 14 *EDX analysis of AlSi10MgCu alloy with 0.15 wt. % Mo + 0.15 wt. % Zr + 0.1 wt. % Co (exact amount of Mo – 0.151 wt. %, Zr – 0.134 wt. %, Co – 0.094 wt. %), without heat treatment - sample D, SEM*

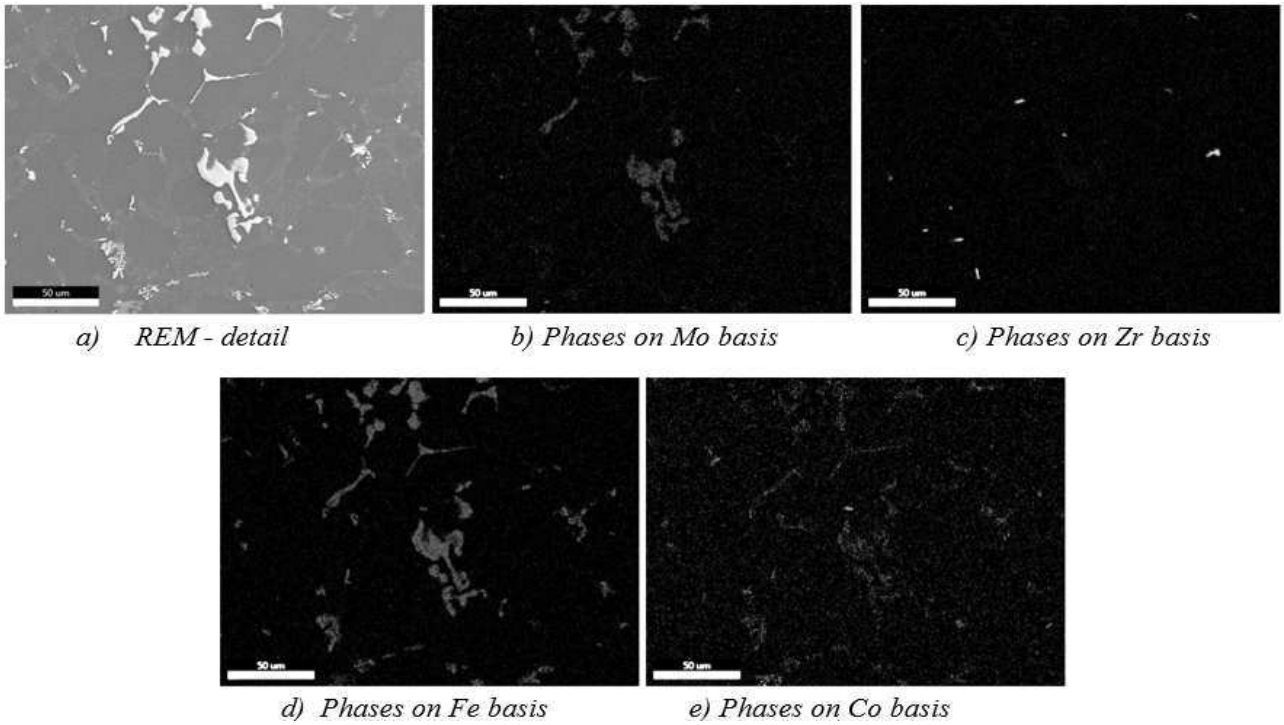

Fig. 15 *Phases mapping of AlSi10MgCu alloy with 0.15 wt. % Mo + 0.15 wt. % Zr + 0.1 wt. % Co (exact amount of Mo – 0.151 wt. %, Zr – 0.134 wt. %, Co – 0.094 wt. %), without heat treatment - sample D, SEM*

AlSi10MgCu + 0.15 wt. % Mo + 0.15 wt. % Zr + 0.1 wt. % Co, sample C, with heat treatment

After the heat treatment, the intermetallic phases were refined (Figure 16) against the alloy without heat treatment (Figure 14). The strontium phase (indicated by the red arrow) and the iron-based phase (indicated by the green arrow) slightly decreased compared to the alloy without heat treatment.

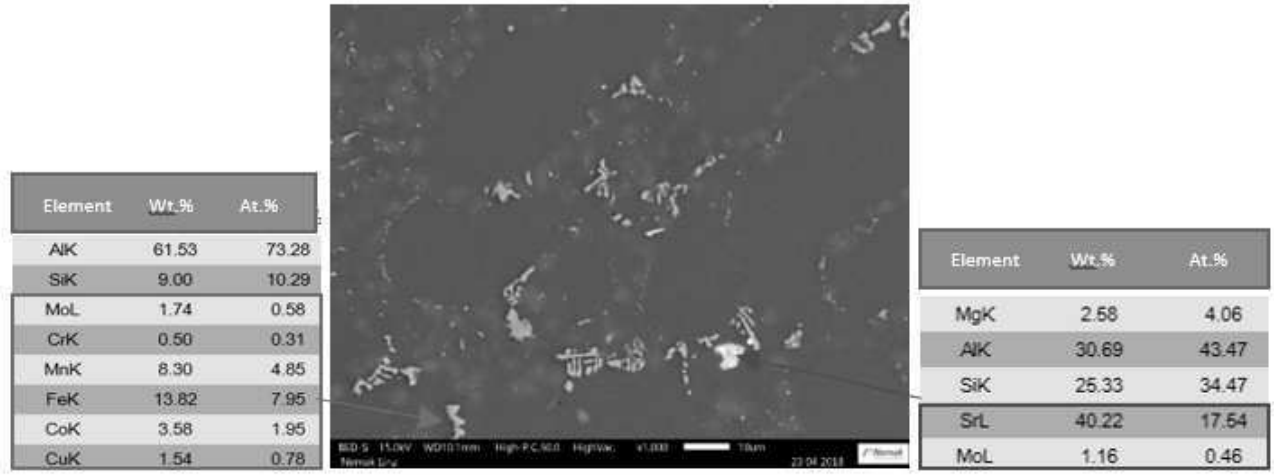

Fig. 16 *EDX analysis of AlSi10MgCu alloy with 0.15 wt. % Mo + 0.15 wt. % Zr + 0.1 wt. % Co (exact amount of Mo – 0.151 wt. %, Zr – 0.134 wt. %, Co – 0.094 wt. %), with heat treatment - sample D, SEM*

Mapping showed a significant Zr-phase reduction after heat treatment, but the Al(Fe, Mn, Mo)Si phase appeared in the form of skeleton formations, and the distribution of Fe, Mn, Mo and Co in small fragmented intermetallic phases (Fig. 17).

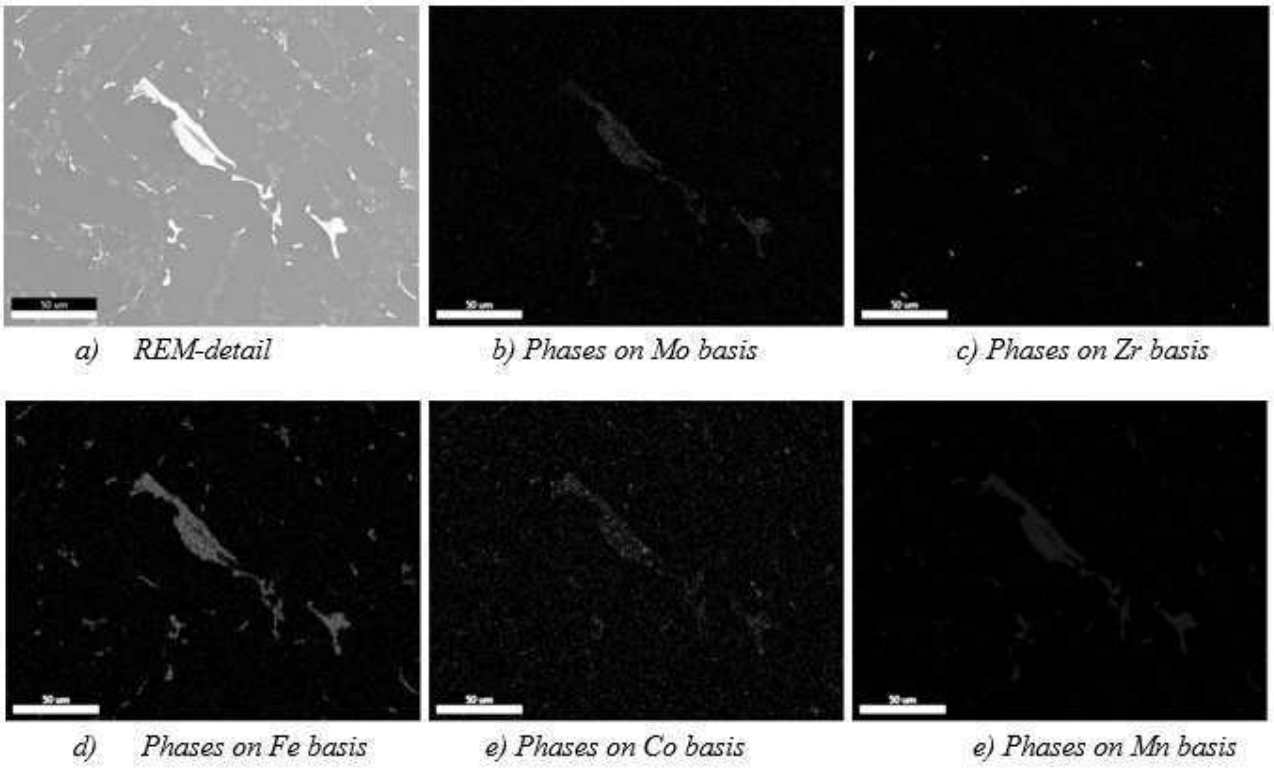

Fig. 17 *Phases mapping of AlSi10MgCu alloy with 0.15 wt. % Mo + 0.15 wt. % Zr + 0.1 wt. % Co (exact amount of Mo – 0.151 wt. %, Zr – 0.134 wt. %, Co – 0.094 wt. %), with heat treatment - sample D, SEM*

4 Conclusion

It can be concluded that molybdenum in the AlSi10MgCu alloy creates skeleton morphology phases with an bound to iron phase Al(Fe, Mn, Mo)Si. The heat treatment has softened these phases and is a prerequisite for increasing the strength characteristics and hardness. By alloying the material with zirconium, the precipitation of Al3Zr phases occurred. These phases represent a strong nucleation potential for α-Al. It has been confirmed that the Al3Zr particles do not tend to interact with other elements (they do not have space for enrichment with other elements) because they are formed just prior to the formation of the α-Al matrix. It has also been observed that cobalt affects the morphology of ferric phases. This shows a limited precipitation effect of transition metals in Al-Si alloys, mainly due to their relatively low solubility in the solid α-Al phase. Even with a synergistic

effect, the transition metals added to the melt caused the formation of a limited number of precipitates, rich in analyzed elements. Precipitates have been distributed inhomogeneously, which may cause a problem in the homogenization of the phases containing transition metals.

It is possible to assume that the transition elements can produce positive high temperature phases, while the heat treatment in the alloy is capable of refining the intermetallic phases.

The findings of this study can provide further insight into the transition metals in Al-Si-Mg-Cu alloys and the possibilities of developing a new generation of heat-resistant Al-Si based alloys.

Acknowledgement:

This work was created as part of the project VEGA grant project no. 1/0494/17. The authors thank the grant agency for their support.

References:

[1] https://www.anubis3d.com/documents/dmls/datasheets/Aluminum-AlSi10Mg.pdf.

[2] RAKHMONOV, J., TIMELLI, J., BONOLLO, F.(2017). Characterization of thr solidification path and microstructure of secondary Al-7Si-3Cu-0.3Mg alloy with Zr,V and Ni additions. *Materials Characterization*, 128, pp. 100–108.

[3] BOLIBRUCHOVA, D., ZIHALOVA, M. (2015). Combined influence of V and Cr on the Al10SiMgMn with a high Fe level.*Materials and technolology*. Vol. 49 Iss.: 5 pp: 681-686.

[4] BOLIBRUCHOVA, D., ZIHALOVA, M. (2014). Vanadium influence on iron based intermatallic phases in Al6Si4Cu. *Archives of metallurgy and materials*. Vol. 59 Iss: 3 pp: 1029-1032.

[5] BOLIBRUCHOVA, D., BRŮNA, M. (2017). Impact of the elements affecting the negative ironbased phases morphology in aluminium alloys - Summary results. *Manufacturing Technology*, Vol. 17, Iss. 5, pp. 675-679.

[6] GAO, T., ZHU, X., SUN, Q., LIU,X. (2013). Morphological evolution of ZrAlSi phase and its impact on the elevated-temperature properties of Al-Si piston alloy, *Journal of Alloys and Compounds*,567:82-88.

[7] MEDVED, J., KORES, S., VONČINA, M. (2018). Development of Innovative Al–Si–Mn–Mg Alloys with High Mechanical Properties, *Light metals*, pp.373-380, DOI: 10.1007/978-3-319-72284-9_50.

[8] VONČINA, M., KORES, S., ERNECL, M., MEDVED, J. (2017). The role of Zr and T6 heat treatment on mickrostruckture evolution and hardness of Alsi9Cu3(Fe). *Journal of Mining and Metallurgy*, Sect. B-Metall. 53 (3) pp. 423-428.

[9] FARKOOSH, A. R., GRANT CHEN, X., PEKGULERYUZ, M. (2015). Interaction between molybdenum and manganese to form effective dispersoids in an Al–Si–Cu–Mg alloy and their influence on creep resistance. *Materials Science & Engineering A* 627, pp.127–138.

[10] BOGDANOFF, T., DAHLE, A.K,SEIFEDDINE, S. (2017). Effect of Co and Ni addition on the microstructure and mechanical properties at room and elevated temperature of an Al-7%Si alloy. *International Journal of Metalcasting* 12(4):1-7.

[11] HAJDUCH, P., BOLIBRUCHOVA, D., DJURDJEVIC, M. (2018). Impact of Molybdenum on the thermal, structural properties and micro hardness of AlSi10Mg(Cu) commercial alloy, *Archives of foundry engineering*, ISSN (1897-3310) Vol. 18 Iss. 3, pp. 19-24.

[12] PASTIRČÁK, T. (2014). Effect of Low Pressure Application during Solidification on Microstructure of AlSi Alloys. In: *Manufacturing technology*. Vol. 14, no. 3, pp. 397-402, ISSN 1213-2489.

[13] BOLIBRUCHOVÁ, D., ŽIHALOVÁ, M. (2013). Possibilities of iron elimination in aluminium alloys by vanadium. In: *Manufacturing technology*. Vol. 13, No. 3, pp. 289-296.

[14] CONEV, M., VASKOVÁ, I., HRUBOVČÁKOVÁ, M., The Influence of Mould Strength on Shrinkage Production for Castings with Different Wall Thickness for Material EN-GJS-400-18LT. In *Manufacturing Technology*, vol. 17., No. 1., pp. 14-18.

[15] HRUBOVČÁKOVÁ, M., VASKOVÁ, I., CONEV, M., BARTOŠOVÁ, M., FUTÁŠ, P. Influence the Composition of the Core Mixture to the Occurrence of Veining on Castings of Cores Produced by Cold-Box-Amine Technology. In *Manufacturing Technology*, vol. 17., No. 1., pp. 39-44.

10.21062/ujep/165.2018/a/1213-2489/MT/18/5/709